Article

Exonuclease I-hydrolysis Assisted Electrochemical Quantitation of Surface-immobilized DNA Hairpins and Improved HIV-1 Gene Detection

Xiaoyi Gao, Xinglin Wang, Yunchao Li, Jiale He, and Hua-Zhong Yu

Anal. Chem., **Just Accepted Manuscript** • DOI: 10.1021/acs.analchem.8b01445 • Publication Date (Web): 08 Jun 2018

Exonuclease I-hydrolysis Assisted Electrochemical Quantitation of Surface-immobilized DNA Hairpins and Improved HIV-1 Gene Detection

Xiaoyi Gao,[†,‡] Xinglin Wang,[†] Yunchao Li,[*,†] Jiale He,[†] and Hua-Zhong Yu[*,‡]

[†]*Department of Chemistry, Beijing Normal University, Beijing 100875, P. R. China*

[‡]*Department of Chemistry, Simon Fraser University, Burnaby, British Columbia V5A 1S6, Canada*

* Corresponding authors: liyc@bnu.edu.cn (Y.L.), hogan_yu@sfu.ca (H.Y.)

ABSTRACT: The complete formation of stem-loop (i.e., hairpin) configuration on chip surface is of particular importance for the application of hairpin DNA (hpDNA) in building biosensors for various analytes with optimized performance. We report herein a convenient electrochemical protocol for evaluating the yield of hairpin DNA conformations upon self-assembly on electrode surface. As of the different hydrolysis capability of Exonuclease I (**Exo I**) towards single-stranded DNA (ssDNA) and hpDNA, we can selectively remove ssDNA from electrode but retain hpDNA strands; based on the changes in the cyclic voltammetric (CV) responses using $[Ru(NH_3)_6]^{3+}$ as redox indicators, we can then determine the fraction of hairpin configurations in mixed DNA self-assembled monolayers (SAMs). It was discovered that the molar fraction of hairpin configuration formed on the surface is considerably lower than that in the binary deposition solution (containing both ssDNA and hpDNA). The accuracy of the Exo I-assisted electrochemical quantitative protocol has been validated by standard DNA hybridization experiments; the relationship between the overall DNA packing density and the yield of hairpin configurations was also evaluated. More importantly, taking HIV-1 gene detection as a trial system, the hpDNA-based biosensor shows significantly improved detection limit and broadened response range upon the background reduction by Exo I-catalyzed hydrolysis.

Keywords: Exonuclease I, DNA hydrolysis, hairpin DNA, surface density, HIV-1 gene detection

INTRODUCTION

A hairpin DNA (hpDNA) is a specially designed single-stranded oligonucleotide with self-complementary stems, which can fold into a stem-loop (i.e., hairpin configuration) under appropriate conditions.[1-3] Benefiting from their unique selectivity to target molecules (such as DNA, proteins, and small molecules),[4-7] hpDNAs have been widely employed as the sensing elements for the construction of chip-based biosensors and other molecular devices,[8-15] which inclusively rely on stimuli-induced conformational switching of substrate-tethered hairpin structures. Therefore, it is particularly important to ensure high formation yield of hairpin configurations when immobilizing such specially designed DNA probes on surface.

It has been confirmed that a hpDNA exists either as a curly single strand, a head-to-tail dimer or a hairpin configuration in solution.[16-18] As a result, the DNA probes with mixed configurations are typically obtained upon immobilization on solid substrates. Clearly, such a DNA self-assembled monolayer (SAM) with mixed configurations may lead to high background signal, which inevitably influence the sensor performance. To solve this issue, efforts have been made to understand the effect of different factors, e.g., probe sequence, stem length, and buffer composition, on the formation and stability of hairpin configurations.[19-23] In addition, different amplification strategies, including enzyme assisted methods[24-26] and hybridization chain reactions[27-31] have been introduced to improve the performance of hpDNA-based sensors lately, which do not involve the reduction of background signal contributed from ssDNA strands. One of the apparent challenges is the lack of convenient methods for quantitatively evaluating the hairpin configurations formed on the substrate surface, i.e., the ratio of hairpin to non-hairpin DNA strands, which is a key factor to the optimized sensor performance.

In retrospect, both cyclic voltammetry (CV) and chronocoulometry (CC) are well-known electrochemical methods for measuring the surface density of DNA immobilized on electrode based on the responses from electrostatically bound redox cations (e.g., $Ru(NH_3)_6^{3+}$).[32,33] However, these conventional electrochemical measurements cannot distinguish the different configurations of surface tethered DNA strands. It is known that Exonuclease I (**Exo I**) from E.coli can catalyze the cleavage of

ssDNA from 3'-terminus in a highly processive manner but does not show any activity to double-stranded DNA (dsDNA).[34-36] Owing to this unique property, we envision that Exo I may have the capability of differentiating ssDNA from hpDNA strands. Combined with Exo I pre-treatment, CV measurements with $Ru(NH_3)_6^{3+}$ may fulfill the function of a quantitation method for the yield of hairpin configurations. More importantly, the pretreatment with Exo I should be also effective in reducing the background signal (*vide supra*).

In this work, we demonstrate an Exo I hydrolysis-assisted electrochemical method (i.e., CV quantitation protocol) for determining the ratio of hairpin configurations in a mixed DNA SAM on electrode. By comparing the amount of DNA nucleotides tethered on electrode (based on the integrated charge of reducing surface bound $[Ru(NH_3)_6]^{3+}$) before and after Exo I-catalyzed cleavage, the ratio of hairpin configuration can be determined accurately. Meanwhile, we have carried out standard DNA hybridization experiments (i.e., selective hybridization with short DNA strands) to validate the accuracy of the Exo I-assisted electrochemical quantitative protocol. Particularly, we have shown that the DNA surface density directly affects the yield of hairpin configurations, and that the reduction of background signal indeed improves the hpDNA-based sensor performance (for which the detection of HIV-1 gene was adapted as a trial system).

EXPERIMENTAL SECTION

Materials and reagents. Tris (hydroxymethyl)-aminomethane (Tris), tris (hydroxymethyl)-aminomethane hydrochloride (Tris-HCl), and 6-mercapto-1-hexanol (MCH) were ordered from Sigma-Aldrich (St. Louis, MO, USA). Hexaammineruthenium (III) chloride ($Ru(NH_3)_6Cl_3$, 98%), tris-(2-carboxyethyl) phosphinehydrochloride (TCEP), silver nitrate ($AgNO_3$), and methyl aldehyde were purchased from Acros (Brussels, Belgium). Exonuclease I (Exo I) was obtained from the Takara Biotechnology Co., Ltd. (Dalian, China). Horseradish peroxidase (HPR)-labeled streptavidin and 3, 3', 5, 5'-tetramethylbenzidine (TMB) were purchased from SeraCare (Gaithersburg, MD, USA) in the format of a ready-to-use reagent kit (H_2O_2 included; Lot No. 10134980). Other general chemicals such as sodium chloride (NaCl), magnesium chloride hexahydrate

($MgCl_2·6H_2O$), sodium carbonate anhydrous (Na_2CO_3), sodium thiosulfate pentahydrate ($Na_2S_2O_3·5H_2O$), sulfuric acid (H_2SO_4, 95–98%), absolute ethanol (C_2H_5OH, ≧99.7%), and nitric acid (HNO_3, >90%) were purchased locally from Beijing Chemical Reagent Co. (Beijing, China).

All oligonucleotides (sequences listed in **Table 1**) were synthesized by Sangon Biotechnology Inc (Shanghai, China) and purified with HPLC. Their stock solutions (100 μM) and all buffer solutions were prepared with deionized water (≥18.2 MΩ cm) produced from a Barnstead Easypure System (Thermo Scientific Inc., Dubuque, USA).

Table 1. Oligonucleotide sequences of hpDNA and ssDNA probes employed in this work.

DNA strand	Sequence
hpDNA-16	$HS(CH_2)_6$O-5'- ACA CGC TCA CTA TGA GAA ACA GCT GGA AAC CGC TCA TAG TGA GCG TGT -3'
ssDNA-48	$HS(CH_2)_6$O-5'- GAC TAA AAG ATA TGA GAA AGA GTC CGT CGA GAG GTC TAG TGA GCG TGT -3'
hpDNA-16-T	5'- ACA CGC TCA CTA TGA GCG GTC TGC AAG TGT TTC TCA TAG TGA GCG TGT -3'
hpDNA-6	$HS(CH_2)_6$O-5'- GCG AGC CTG GGA TTA AAT AAA ATA GTA AGA ATG TAT AGC GCT CGC -biotin -3'
HIV-1	5'- GCT ATA CAT TCT TAC TAT TTT ATT TAA TCC CAG -3'
Target-10	5'- ACA CGC TCA C -3'

Polyacrylamide gel electrophoresis (PAGE) assay. A 20% native polyacrylamide gel was prepared to examine the hydrolysis behavior of Exo I towards solution-dispersed DNA strands with different configurations. For each lane of the gel, 10 μL of DNA sample (1.5 μM) was loaded. Electrophoresis was carried out at 100 V for 90 min at room temperature in 1×TB buffer (89 mM Tris–borate, pH 8.3). Afterwards, the gel was immersed in a freshly prepared stain-all solution

(containing 0.3 g of silver nitrate, 200 μL of formaldehyde, 200 mL of H_2O) for 30 min. Subsequently, the gel was incubated in the developer solution (4.5 g of sodium carbonate anhydrous, 200 μL of formaldehyde, 40 μL of sodium thiosulfate of 10 mg/ml, 200 mL of H_2O) for 5 ~ 10 min. After washing with distilled water for three times, the PAGE results were photographed using a digital camera (Nikon, D7100).

Preparation of DNA-modified gold electrodes. Gold disk electrodes (2.0 mm in diameter) were polished with 0.3 μm Al_2O_3 powder and carefully rinsed with deionized water and ethanol (three times each), respectively. Afterwards, they were electrochemically cleaned in 1.0 M H_2SO_4 solution by cycling the potential between -0.2 and 1.6 V (vs. Ag|AgCl) until a stable CV was obtained. The cleaned electrodes were rinsed thoroughly with deionized water and blown dry with high-purity N_2. The thiolated DNA (freshly prepared) of different concentrations in 10 mM Tris coupling buffer (containing 150 mM NaCl, 50 mM $MgCl_2$, pH = 7.4) were heated to 80 °C for 5 min followed by slowly cooling to room temperature (25 °C). The cleaned electrodes were immersed in 100 μL of thus-prepared thiolated DNA solution for 4 h. After immobilization, the electrodes were rinsed with 10 mM Tris buffer, and then incubated in 1.0 mM MCH for 1.0 h, and thoroughly rinsed with 10 mM Tris buffer prior to electrochemical measurements. For HIV-1 gene detection, the electrodes modified with biotinylated stem-loop probes (hpDNA-6) were first incubated with HPR-labeled-streptavidin (5.0 μg/mL) for 10 min at room temperature. After removing the nonspecifically adsorbed HRP through washing with deionized water, the electrodes were then examined through amperometric measurements.

Exo I-assisted DNA hydrolysis. The stock Exo I solution (1.25 U/μL, unless otherwise stated) was prepared in a buffer of 67 mM glycine-KOH (pH 9.5), 67 mM $MgCl_2$ and10 mM DTT. For DNA hydrolysis in solution, 2.0 μL of 10 μM DNA (ssDNA, dsDNA, and hpDNA) were added into 18 μL of the Exo I solution and incubated at 37 °C for 30 min. For surface experiments, the DNA-modified gold electrode was immersed in 80 μL of the Exo I solution at 37 °C for 3 h (unless otherwise stated).

Electrochemical characterization. CV and amperometric measurements were performed at room temperature with a Zahner Zennium electrochemical workstation (Kronach, Germany) with a conventional three-electrode cell consisting of an Ag|AgCl (3.0 M NaCl) reference electrode, a

platinum wire counter electrode, and a gold working electrode (modified with DNA strands as described above). All CV measurements were performed in 10 mM Tris buffer (pH 7.4) containing 5.0 μM $[Ru(NH_3)_6]Cl_3$. The electrolyte solutions were deoxygenated with N_2 for 12 min in advance and kept under N_2 atmosphere throughout the measurements. The cathodic peak of the first scan was integrated to estimate the amount of DNA on the electrode.[33] The amperometric detection using TMB as the redox indicator was performed at a fixed potential of -100 mV (vs. Ag|AgCl) and a steady state was reached and recorded within 300 s.

RESULTS AND DISCUSSION

Exo I-assisted cleavage of DNA strands in solution. As mentioned above, Exo I can cleave ssDNA progressively and does not show any activity towards double-stranded DNA (dsDNA) in solution.[34-36] We have recently investigated the Exo I-assisted hydrolysis of DNA self-assembled monolayers (SAMs), and demonstrated that it can cleave surface-tethered ssDNA (independent of packing density and base sequences) as well.[37] As "control" experiments, we have run polyacrylamide gel electrophoresis assays (PAGE) to examine the hydrolysis behavior of Exo I towards solution-dispersed DNA strands with different configurations (i.e., ssDNA, dsDNA, and hpDNA). As shown in Figure 1, the clear band observed in Lane 1 is ssDNA-48 without Exo I treatment. The original band essentially disappeared in the presence of Exo I (1.25 and 1.5 U/μL; lanes 2 and 3), confirming that solution-dispersed ssDNA strands can be hydrolyzed completely with Exo I. The bands observed on lane 4 to lane 7 are corresponding to dsDNA; these bands did not change at all with the same amounts of Exo I added, indicating that Exo I does not show any activity towards dsDNA. More importantly, the bands corresponding to hpDNA-16 (lane 7 to 10) also remain unchanged when Exo I was added at an even higher concentration (2.0 U/μL). The reason why Exo I cannot hydrolyze hpDNA-16 strands is attributed to the protection effect from the dsDNA-like complementary stems (ΔG = - 21.07 kcal/mol).[38] These PAGE results confirmed that Exo I indeed has the ability to differentiate ssDNA from hpDNA strands in solution.

Exo I-assisted electrochemical protocol for quantifying surface-tethered hpDNA. Based on

the different hydrolysis behavior of Exo I towards ssDNA and hpDNA, we explored the feasibility of using CV measurements in the presence of 5.0 μM $[Ru(NH_3)_6]^{3+}$ under low ionic strength (10 mM Tris buffer) to quantitate the ratio of hairpin configurations in mixed hpDNA-16/ssDNA-48 SAMs on gold. Such a convenient electrochemical quantitation method has been validated previously for determining the surface density of DNA strands immobilized on electrode surface, which is based on the integrated charge corresponding to the reduction peak of electrostatically bound $[Ru(NH_3)_6]^{3+}$, while the contributions form solution diffused species minimized.[33]

With the above-mentioned protocol, we systemically evaluated the molar fraction of the hairpin confirmation formed in the mixed hpDNA-16/ssDNA-48 and hpDNA-16 SAMs on gold. Figure 2 shows representative CV curves of surface-tethered DNA strands with distinct configurations (right insets). At first, clear-cut, near symmetric CV peaks for the $[Ru(NH_3)_6]^{3+/2+}$ redox process on as-formed DNA SAM-modified gold electrode were all observed. Upon Exo I-assisted hydrolysis, the CV peaks for electrodes modified with ssDNA-48 eventually vanished (Figure 2a); in contrast the CVs for electrodes modified with hpDNA-16 strands shown in Figure 2c are relatively stable besides differences in the capacitive currents. It is important to notice that for a mixed ssDNA-48/hpDNA-16 film (Figure 2b), we have observed significant decrease in the redox peaks; however, they are still distinct upon the Exo I-assisted hydrolysis. Considering the fact that Exo I does not show any activities towards hpDNA-16 in solution, we believe that the decrease in the redox peaks corresponds to the amount of ssDNA strands on the surface. The fraction of ssDNA-48 and hpDNA-16 strands (of hairpin conformation) on the electrode surface, therefore, can be calculated based on:

$$\chi_{ss} = [(Q_{int} - Q_{fin})/0.7] / Q_{int} \times 100\% \quad (1)$$

$$\chi_{hp} = [Q_{int} - (Q_{int} - Q_{fin})/0.7] / Q_{int} \times 100\% \quad (2)$$

where Q_{int} and Q_{fin} are the integrated charges before and after the Exo I catalyzed hydrolysis, respectively. The value of 0.7 is the hydrolysis efficiency of Exo I toward surface-immobilized ssDNA with 48 mer, which was determined by the length of DNA fragments after Exo I-assisted hydrolysis.[37]

The relationship between the molar ratio of surface-tethered hpDNA-16 and that in the binary deposition solution is shown in Figure 3. While the fraction of hpDNA-16 on surface increases monotonically with its increased concentration in solution, it is evident that the surface composition is different from that in solution. Particularly, the fraction of hpDNA-16 on surface is substantially less than that in the deposition solution, indicative of higher affinity of ssDNA towards gold surface in comparison with hpDNA. The fact that a hpDNA has a loop conformation may lead to a sluggish kinetics when competes with unstructured DNA single strands.[39-41]

To confirm the above obervations, we have carried out DNA hybirdization experiments to quantitate the hairpin ratio of surface-confined hpDNA-16/ssDNA-48 SAMs (Supporting Information, Figure S2 and S3). Particularly we have chosen a short DNA strand (Targrt-10, with 10 nucleotides) that can hybridize with the ssDNA-48 strands and should not open the hairpin configurations (hpDNA-16). In this case, the amount of ssDNA-48 strands on surface can be determined from the increase in the CV peaks when measrued with $[Ru(NH_3)_6]^{3+}$. As shown in Figure 4, the fractions of hairpin configurations of surface-confined hpDNA-16/ssDNA-48 SAMs measured by the DNA hybirdization method are consistent with those determined by the Exo I hydrolysis approach decribed above. The best liner fit to the correlation plot between the two sets of data yeilds a slope of 1.00 with a R^2 value of 0.990, which further validates the Exo I assisted electrochemical method for the quantitation of hpDNA configurations on surface. The other important finding is that even with only hpDNA-16 strands in solution, the assembled surface only contains 76 ± 4% hpDNA-16 hairpins (as evidenced in both Figure 3 and Figure 4); the exact reason certainly deserves further investigations, but we suspect that the assembly process may induce the restructuring of these hairpin conformations. Another important factor we should consider is the overall surface density of DNA strands on retaining hpDNA conformations; we therefore, systematically studied the correlation between the fraction of hpDNA strands and the overall surface density. To be more related to sensor applications we have chosen a hpDNA with 6 complementary stem (hpDNA-6). As shown in Figure 5, we have observed a clear decrease in the surface fraction of hpDNA-6 when the total surface density increases. For probe densities below $\sim 2\times10^{12}$ molecules/cm^2, the hairpin yields can reach as high as 90% (consisent with

the results presented above). As the DNA strands pack more densely, their hairpin yield decreases remarkably; for a high surface density (e.g., 15×10^{12} molecules/cm^2), it decreases to be as low as 11%.

Exo I-assisted background reduction for improved HIV-1 gene detection. The consistency of the above experiments to validate the Exo I-assisted electrochemical quantitation of hpDNA configurations on surface encouraged us to apply these findings in a practical sensor setting, i.e., the detection of HIV-1 gene with hpDNA probes.[42,43] Additonal fluorescence spectroscopy experiments revealed that hpDNA with a 6-complementary stem shows the best performance to HIV-1 gene targets (Supporting Information, Figure S4). As described above, the fraction of hpDNA configuration can only reach 90% even at at low overall probe density, indicating that hpDNA-based biosensors are inevitably accompanied with high background signals generated by non-hairpin configurations. Therefore, it is of great significance to eliminate the influence of non-hairpin configurations in order to improve their detection performance. To demonstrate the background reduction effect of Exo I-assisted hydrolysis, we fabricated hpDNA-6-based sensors for HIV-1 gene detection and employed amperometric measurements to test their perfromance with and without background reduciton. As shown in Scheme I, hpDNA-6 strands dually labeled with a thiol and a biotin moiety at the 5'- and 3'-end were immobilized onto the gold surface; the transducion of electrochemical signals relies on the binding of streptavidin-horseradish peroxidase (HRP) conjugates, which in turn catalyzes the reduciton of H_2O_2 in the presence of TMB. Initially, the immobilized hpDNA-6 probe was in the "closed" state (hairpin conformation) in the absence of HIV-1 gene, which shielded biotin from being approached by rather bulky streptavidin-HRP conjuates due to the steric effect (Scheme Ia). After hybridization, the loop sequence formed a rigid duplex with the HIV-1 target, thus relocating the biotin away from the electrode surface to allow for the binding of streptavidin-HRP conjuates (Scheme Ic). However, the existence of ssDNA on the surface can allow the binding of streptavidin-HRP conjuates in the absence of HIV-1 gene, thus leading to high background signal (i.e., causing false postive responses). We envision that the introduction of Exo I can effectively reduce the background signals by cleaving ssDNA strands.

In Figure 6, we have shown the amperometric responses of such a sensor before (a) and after (a′) Exo I-assisted background reduction. As particularly shown in Figure 6(a) as the dashed line, the background current (i.e., without the presence of HIV-1 targets) decreased significantly. In both cases, the steady state current obtained increases upon adding different concentrations of the HIV-1 targets (as listed in the corresponding plot), which are depicted in the plots of ΔI (difference between sample and

background currents) as function of the target DNA concentrations (Figure 6b, 6b′). These working (calibration) curves are unfortunately not linear, but show impressive sensitivities at low concentration ranges (< 10 nM). To better illustrate the detection limits and dynamic response ranges, in Figure 6c and 6c′ we have plotted ΔI value with respect to the logarithm of the target DNA concentration. Without the background reduction, the plot exhibits a linear correlation from 10 pM to 50 nM with a R^2 value of 0.992. Meanwhile, the linear response range upon Exo I-assisted background reduction is from 100 fM to 10 nM with a R^2 value of 0.998. The detection limit without and with Exo I-catalyzed hydrolysis were calculated to be 18 pM and 150 fM, respectively, according to the "$3\sigma/b$" rule (where σ is the standard deviation of the y-intercept of the regression line and b is the slope with appropriate propagation of experimental uncertainties).[44]

Table 2. Comparison of various assay methods for the detection of HIV-1 gene.

Detection method	LOD	Response range	Ref.
Fluorescence	3 nM	7 nM-80 nM	42
Fluorescence	0.29 nM	5 nM-100 nM	43
Square Wave Voltammetry	10 pM	20 nM-100 nM	45
Differential Pulse Voltammetry	5 nM	40 nM-2.56 μM	46
Electrochemical Impedance Spectroscopy	30 pM	100 pM-300 nM	47
Differential Pulse Voltammetry	1 pM	1.5 pM-50 pM	48
Amperometry	18 pM	10 pM-50 nM	This study without Exo I
Amperometry	150 fM	100 fM-10 nM	This study with Exo I

As mentioned above, the detection of HIV-1 gene has been extensively investigated in the past two decades due to its practical importance in the early detection of Acquired Immunodeficiency Syndrome

(AIDS). In Table 2, we have listed the detection performance of our hpDNA-based HIV-1 sensors for a direct comparison with previous spectroscopic and electrochemical studies.[42-43,45-48] We note that without the Exo-I assisted background reduction, both the detection limit and the dynamic response range are comparable with other hpDNA-based HIV-1 electrochemical sensors, and slightly better than those fluorescence detection.[42,43] Upon introducing Exo I-catalyzed hydrolysis to reduce the background signals from ssDNA strands, the hpDNA-based biosensor shows a much better detection performance with a lower detection limit (150 fM) and a broad linear response range (100 fM –10 nM).

It should be emphasized that the hpDNA sensors we have examined above for the HIV-1 gene detection is merely a trial system to demonstrate the effect of Exo I-assisted background reduction. The capability of our convenient electrochemical quantitation in conjunction with Exo I hydrolysis-assisted conformational differentiation is unlimited; in principle any other DNA sensor constructs (e.g., folded aptamers, G-quadruplexes, i-motifs, and three-way/four-way junctions) can be readily improved by introducing Exo I-catalyzed hydrolysis to remove the unwanted DNA single strands.

CONCLUSION

In summary, we developed a convenient Exo I hydrolysis-assisted electrochemical protocol to evaluate the yield of hairpin configurations upon the immobilization of DNA probes on electrode surface. Particularly, the combined Exo I-assisted hydrolysis and DNA hybridization experiments have validated that the ratio of hairpin configuration formed on the surface is appreciably lower than that in the binary assembly solution, which significantly decreases upon increasing the overall probe density on the surface. More importantly, it was demonstrated that the background signal caused by non-hairpin DNA strands can be reduced by Exo I-catalyzed hydrolysis, thus improving the detection performance for hpDNA-based sensors; in particular the sensor for HIV-1 gene detection adapted as the trial system shows a 120-fold improvement in the detection limit. It should be emphasized that the developed electrochemical quantitation protocol in conjunction with the background reduction with Exo I assisted hydrolysis can be adapted to many other biosensors with designed DNA constructs to achieve their optimized performance.

Acknowledgements

This work was jointly supported by the National Natural Science Foundation of China (NSFC, 21573024, 21273020, 21003012, and State Key Program 21233003), Beijing Natural Science Foundation (2182026), Beijing Science and Technology New Star Project (2010B021), Scientific Research Foundation for Returned Scholars of Ministry of Education of China, and Natural Science and Engineering Council of Canada (NSERC)

Supporting Information

Additional experimental results for validating the Exo I hydrolysis-assisted electrochemical quantitation method; hybridization results for quantifying the yield of hairpin configurations of hpDNA-16-modified electrodes; fluorescence spectroscopy data for optimizing the stem length of hpDNA probes designed for HIV-1 gene detection; recovery test for HIV-1 targets in biological samples. This material is available free of charge via the Internet at http://pubs.acs.org.

References

(1) Tyagi, S.; Kramer, F. R. *Nat. Biotechnol.* **1996**, *14*, 303–308.

(2) Bonnet, G.; Krichevsky, O.; Libchaber, A. *Proc. Natl. Acad. Sci. U.S.A.* **1998**, *95*, 8602–8606.

(3) Tsourkas, A.; Behlke1, M. A.; Rose1, S. D.; Bao, G. *Nucleic Acids Res.* **2003**, *31*, 1319–1330.

(4) Riccelli, P. V.; Merante, F.; Leung, K. T.; Bortolin, S.; Zastawny, R. L.; Janeczko, R.; Benight, A. S. *Nucleic Acids Res.* **2001**, *29*, 996-1004.

(5) Fan, C.; Plaxco, K. W.; Heeger, A. J. *Proc. Natl. Acad. Sci.* **2003**, *100*, 9134-9137.

(6) Xiao, Y.; Lai, R. Y.; Plaxco, K. W. *Nat. Protoc.* **2007**, *2*, 2875-2880.

(7) Liu, G.; Wan, Y.; Gau, V.; Zhang, J.; Wang, L.; Song, S.; Fan, C. *J. Am. Chem. Soc.* **2008**, *130*, 6820-6825.

(8) Song, S.; Liang, Z.; Zhang, J.; Wang, L.; Li, G.; Fan, C. *Angew. Chem. Int. Ed.* **2009**, *48*, 8670 –8674.

(9) Jayagopal, A.; Halfpenny, K. C.; Perez, J. W.; Wright, D. W. *J. Am. Chem. Soc.* ***2010***, *132*, 9789–9796.

(10) Wei, F.; Wang, J.; Liao, W.; Zimmermann, B. G.; Wong, D. T.; Ho, C. M. *Nucleic Acids Res.* **2008**,

36, e65.

(11) He, X.; Wang, G.; Xu, G.; Zhu, Y.; Chen, L.; Zhang, X. *Langmuir* **2013**, *29*, 14328−14334.

(12) Ren, K.; Wu, J.; Ju, H.; Yan, F. *Anal. Chem.* **2015**, *87*, 1694−1700.

(13) Xiong, E.; Li, Z.; Zhang, X.; Zhou, J.; Yan, X.; Liu, Y.; Chen, J. *Anal. Chem.* **2017**, *89*, 8830−8835.

(14) Jiang, X.; Wang, H.; Wang, H.; Zhuo, Y.; Yuan, R.; Chai, Y. *Anal. Chem.* **2017**, *89*, 4280−4286.

(15) Jung, C.; Allen, P. B.; Ellington, A. D. *ACS Nano*. **2017**, *11*, 8047−8054.

(16) Mukerji, I.; Shiber, M. C.; Fresco, J. R.; Spiro, T. G. *Nucleic Acids Res.* **1996**, *24*, 5013–5020.

(17) Dornberger, U.; Behlke, J.; Birch-Hirschfeld, E.; and Fritzsche, H. *Nucleic Acids Res.* **1997**, *25*, 822–829.

(18) Trauger, J. W.; Baird, E. E.; Dervan, P. B. *Angew. Chem. Int. Ed.* **1998**, *37*, 1421–1423.

(19) Tsourkas, A.; Behlke, M. A.; Rose, S. D.; Bao, G. *Nucleic Acids Res.* **2003**, *31*,1319–1330.

(20) Lubin, A. A.; Hunt, B. V. S.; White, R. J.; Plaxco, K. W. *Anal. Chem.* **2009**, *81*, 2150–2158.

(21) Huang, C.; Stakenborg, T.; Cheng, Y.; Colle, F.; Steylaerts, T.; Jans, K.; Dorpe, P. V.; Lagae, L. *Biosens. Bioelectron.* **2011**, *26*, 3121–3126.

(22) Bockisch, B.; Grunwald, T.; Spillner, E.; Bredehorst, R. *Nucleic Acids Res.* **2005**, *33*, e101.

(23) Shi, X.; Wen, J.; Li, Y.; Zheng, Y.; Zhou, J.; Li, X.; Yu, H.-Z. *ACS Appl. Mater. Interfaces*. **2014**, *6*, 21788−21797.

(24) Xiong, E.; Zhang, X.; Liu, Y.; Zhou, J.; Yu, P.; Li, X.; Chen, J. *Anal. Chem.* **2015**, *87*, 7291−7296.

(25) Wang, Y.; Bai, X.; Wen, W.; Zhang, X.; Wang, S. *ACS Appl. Mater. Interfaces*. **2015**, *7*, 18872−18879.

(26) Shi, X.-M.; Fan, G.-C. Shen, Q.; Zhu, J. *ACS Appl. Mater. Interfaces*. **2016**, *8*, 35091−35098.

(27) Huang, J.; Wu, Y.; Chen, Y.; Zhu, Z.; Yang, X.; Yang, C. J.; Wang, K.; Tan, W. *Angew. Chem. Int. Ed.* **2011**, *50*, 401–404.

(28) Li, B.; Jiang, Y.; Chen, X.; Ellington, A. D. *J. Am. Chem. Soc.* **2012**, *134*, 13918−13921.

(29) Bi, S.; Chen, M.; Jia, X.; Dong, Y.; Wang, Z. *Angew. Chem. Int. Ed.* **2015**, *54*, 8144 –8148.

(30) Wu, C.; Cansiz, S.; Zhang, L.; Teng, I.-T.; Qiu, L.; Li, J.; Liu, Y.; Zhou, C.; Hu, R.; Zhang, T.; Cui, C.; Cui, L.; Tan, W. *J. Am. Chem. Soc.* **2015**, *137*, 4900−4903.

(31) Su, F.-X.; Yang, C.-X.; Yan, X.-P. *Anal. Chem.* **2017**, *89*, 7277−7281.

(32) Steel, A. B.; Herne, T. M.; Tarlov, M. J. *Anal. Chem.* **1998**, *70*, 4670−4677.

(33) Yu, H.-Z.; Luo, C.-Y.; Sankar, C. G.; Sen, D. *Anal. Chem.* **2003**, *75*, 3902−3907.

(34) Lehman, I. R. *J. Biol. Chem.* **1960**, *235*, 1479−1487.

(35) Breyer, W. A.; Matthews, B. W. *Nat. Struct. Biol*. **2000**, *7*, 1125−1128.

(36) Korada, S. K. C.; Johns, T. D.; Smith, C. E.; Jones, N. D.; McCabe, K. A.; Bell C. E. *Nucleic Acids Res.* **2013**, *41*, 5887–5897.

(37) Gao, X.; Geng, M.; Li, Y.; Wang, X.; Yu, H.-Z. *Anal. Chem.* **2017**, *89*, 2464−2471.

(38) OligoAnalyzer 3.1 | IDT http://www.idtdna.com/calc/analyzer (accessed Apr 26, 2018)

(39) Moiseev, L.; Unlu, M. S.; Swan, A. K.; Goldberg, B. B.; Cantor, C. R. *Proc. Natl. Acad. Sci.* **2006** ,*103*, 2623–2628.

(40) Ambia-Garrido, J.; Vainrub, A.; Pettitt, B. M. *Comput. Phys. Commun.* **2010**, *181*, 2001–2007.

(41) Steichen, M.; Buess-Herman, C. *Electrochem Commun.* **2005**, *7*, 416−420.

(42) Chen, L.; Song, L.; Zhang, Y.; Wang, P.; Xiao, Z.; Guo, Y.; Cao, F. *ACS Appl. Mater. Interfaces* **2016**, *8*, 11255−11261.

(43) Zhao, H.; Wang, L.; Zhu, J.; Wei, H.; Jiang, W. *Talanta* **2015**, *138*, 163−168.

(44) Harris, D. C. Quantitative Chemical Analysis, 9th Ed.; W. H. Freeman and Co.; 2016; pp 102−104.

(45) Zhang, D.; Peng, Y., Qi, H.; Gao, Q.; Zhang, C. *Biosens. Bioelectron.* **2010**, *25*, 1088−1094.

(46) Li, B.; Li, Z.; Situ, B.; Dai, Z.; Liu, Q.; Wang, Q.; Gu, D.; Zheng, L. *Biosens. Bioelectron.* **2014**, *52*, 330−336.

(47) Poorghasem, R.; Saberi, R. S.; Shayan, M.; Mehrgardi, M. A.; Kiani, A. *Electrochim. Acta* **2016,** *222*, 1483−1490.

(48) Sun, A.-L.; Jia, F.-C.; Zhang, Y.-F.; Wang, X.-N. *Analyst* **2015**, *140*, 2634−2637.

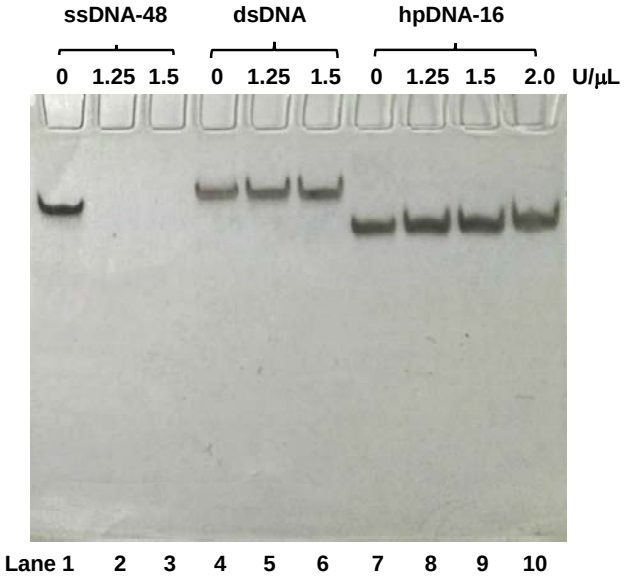

Figure 1. Native PAGE of different DNA strands after Exo I hydrolysis for 30 min at 37 °C. The gel was stained with silver nitrate for visualization. Lane 1 to 3: 10 μM ssDNA-48 treated with Exo I (0, 1.25, and 1.50 U/μL, respectively); Lane 4 to 6: 10 μM dsDNA with Exo I (0, 1.25, and 1.50 U/μL, respectively); Lane 7 to 10: 10 μM hpDNA-16 with Exo I (0, 1.25, 1.50, and 2.00 U/μL, respectively).

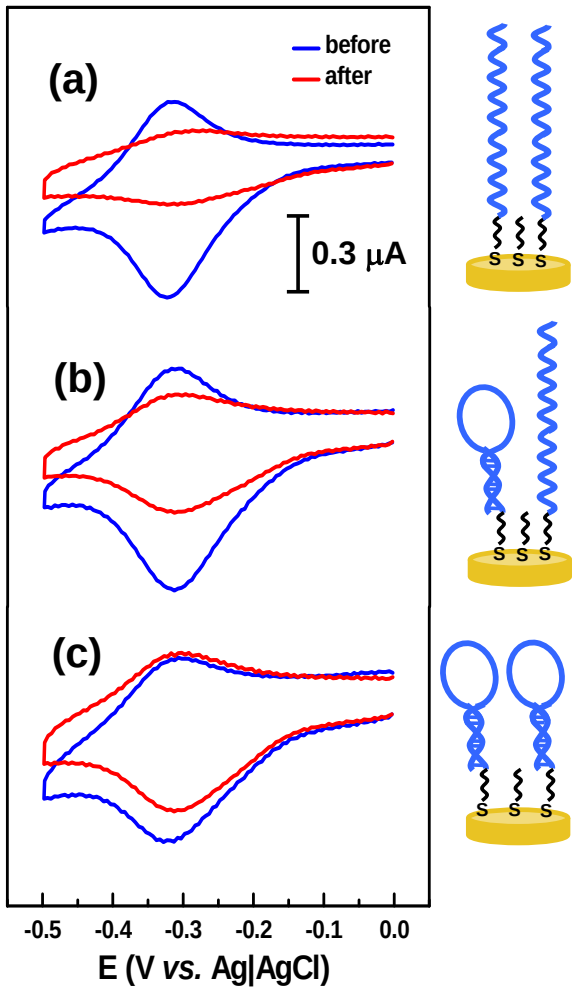

Figure 2. Representative CV responses of gold electrodes modified with (a) ssDNA-48, (b) 1:1 ratio of hpDNA-16 and ssDNA-48, and (c) hpDNA-16, in 10 mM Tris buffer in the presence of 5.0 μM $[Ru(NH3)_6]Cl_3$ before and after hydrolysis with 1.25 U/μL Exo I for 3 h at 37 °C. The right insets show the schematic configurations of DNA-modified electrodes, respectively.

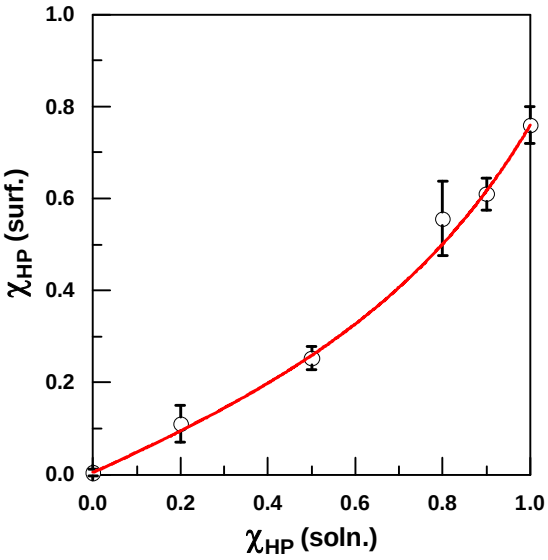

Figure 3. Molar fraction of surface-tethered hpDNA-16 as function of the solution composition. The solid line is to guide the eyes only, and the error bars are standard deviations from three replicated experiments.

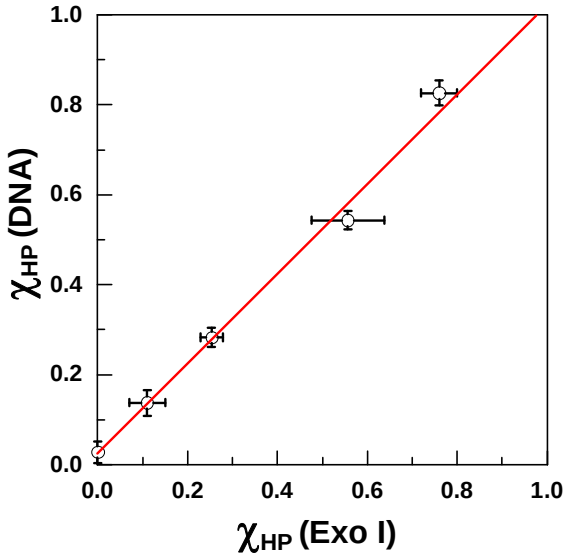

Figure 4. Correlation between the molar fractions of surface-tethered hpDNA-16 measured by Exo I hydrolysis and DNA hybridization. The solid line shows the best linear fit to the experimental data.

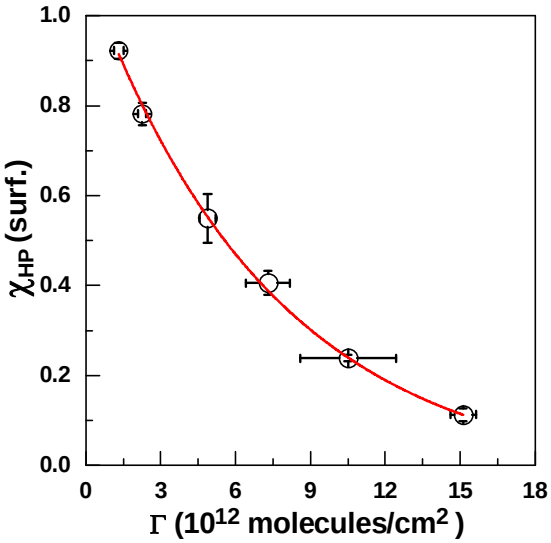

Figure 5. Molar fraction of surface-tethered hpDNA-6 as function of the overall surface density. The error bars represent standard deviations determined from three replicated experiments. The solid line is to guide the eyes only.

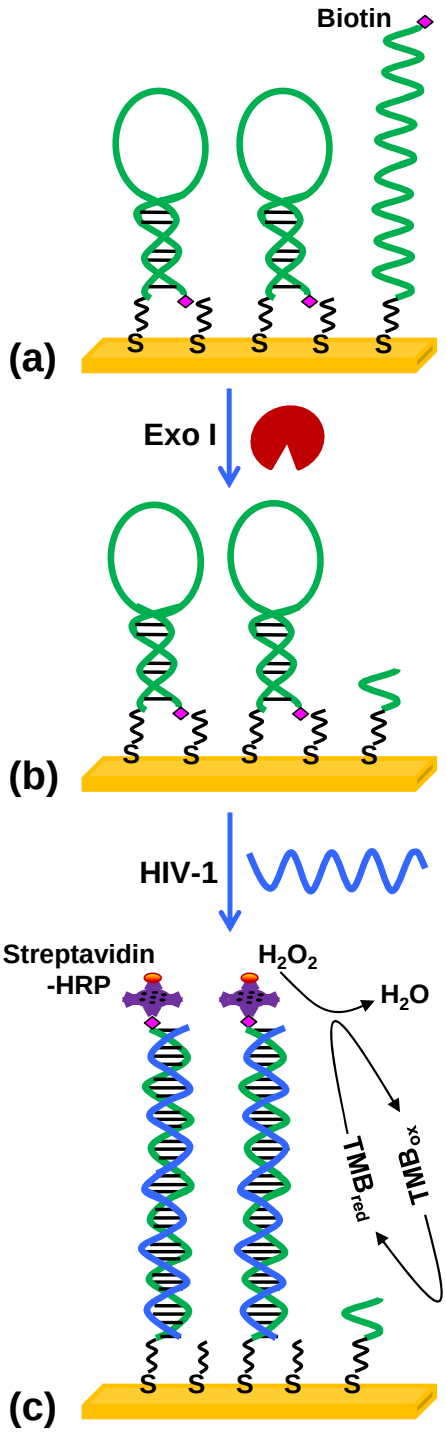

Scheme I. Schematic view of Exo I hydrolysis-assisted hpDNA biosensors. (a) hpDNA- based sensor in the presence of ssDNA strands. (b) Exo I catalyzed hydrolysis of ssDNA strands that are accessible of HRP binding to reduce background signal. (c) Upon hybridization with HIV-1 gene, the formation of duplex make the biotin accessible for HRP binding, which catalyzes the electrochemical reduction of hydrogen peroxide.

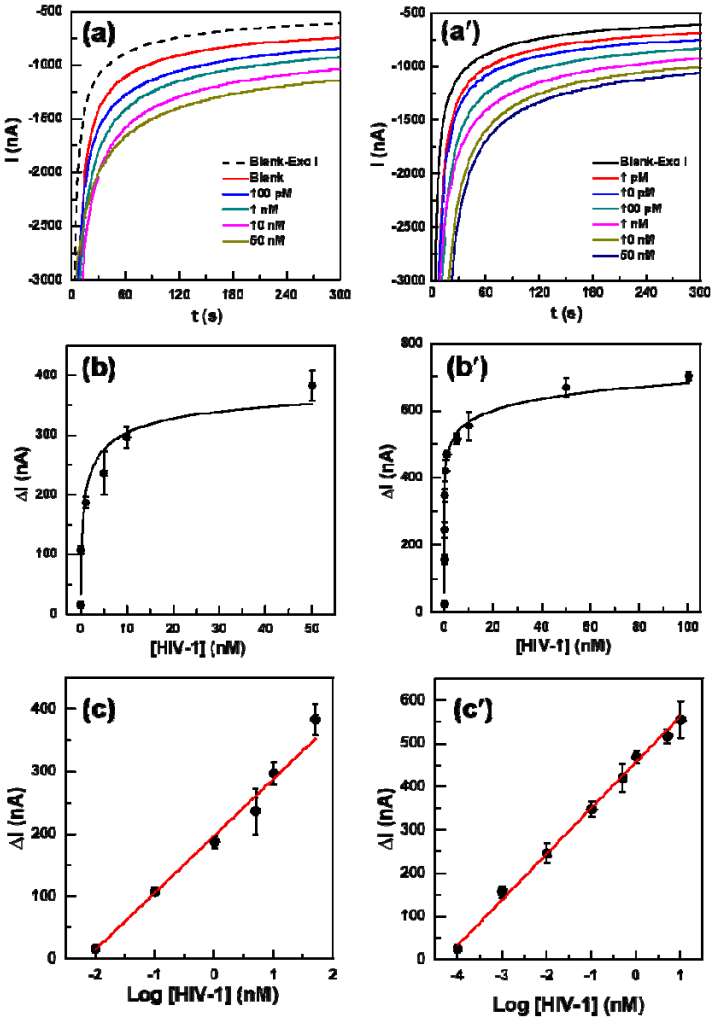

Figure 6. Amperometric response for different concentrations of HIV-1 targets without (a) and with (a′) Exo I catalyzed hydrolysis. (b) and (b′) show ΔI (difference between signal and background current) as function of the target DNA concentrations. (c) and (c′) show the plots of linear relationship between the ΔI values with respect to the logarithm of the target DNA concentration. The solid lines are the linear fit of the experimental data, the R^2 values equal to 0.992 and 0.998 for (c) and (c′), respectively. Error bars represent standard deviations obtained from three independent experiments.

For TOC only